1.54-μm TM-mode waveguide optical isolator based on the nonreciprocal-loss phenomenon: device design to reduce insertion loss

T. Amemiya,[1,2,*] H. Shimizu,[3] M. Yokoyama,[4] P. N. Hai,[4] M. Tanaka,[4] and Y. Nakano[1,2]

[1]Research Center for Advanced Science and Technology, The University of Tokyo, 4-6-1 Komaba, Meguro-ku, Tokyo 153-8904, Japan

[2]Solution Oriented Research for Science and Technology, Japan Science and Technology Agency, Kawaguchi Center Building, 4-1-8 Honcho, Kawaguchi-shi, Saitama 332-0012, Japan

[3]Department of Electrical and Electronic Engineering, Tokyo University of Agriculture and Technology, 2-24-16 Nakacho, Koganei, Tokyo 184-8588, Japan

[4]Department of Electronic Engineering, The University of Tokyo, 7-3-1 Hongo, Bunkyo-ku, Tokyo 113-8656, Japan

*Corresponding author: ametomo@hotaka.t.u-tokyo.ac.jp

Received 22 January 2007; accepted 25 April 2007;
posted 3 May 2007 (Doc. ID 79258); published 8 August 2007

We developed a 1.5-μm band TM-mode waveguide optical isolator that makes use of the nonreciprocal-loss phenomenon. The device was designed to operate in a single mode and consists of an InGaAlAs/InP ridge-waveguide optical amplifier covered with a ferromagnetic MnAs layer. The combination of the optical waveguide and the magnetized ferromagnetic metal layer produces a magneto-optic effect called the nonreciprocal-loss phenomenon—a phenomenon in which the propagation loss of light is larger in backward propagation than it is in forward propagation. We propose the guiding design principle for the structure of the device and determine the optimized structure with the aid of electromagnetic simulation using the finite-difference method. On the basis of the results, we fabricated a prototype device and evaluated its operation. The device showed an isolation ratio of 7.2 dB/mm at a wavelength from 1.53 to 1.55 μm. Our waveguide isolator can be monolithically integrated with other waveguide-based optical devices on an InP substrate. © 2007 Optical Society of America

OCIS codes: 230.3810, 230.3240, 250.5980.

1. Introduction

The photonic integrated circuit that combines various optoelectronic devices on a semiconductor substrate is an indispensable component for constructing functional optical-communication networks. To make these types of photonic integrated circuits, we need to develop optical isolators that can be monolithically combined with waveguide-based optical devices. This paper reports one type of optical isolator: a semiconductor waveguide isolator based on a magneto-optic phenomenon called the nonreciprocal-loss phenomenon.

Optical isolators are indispensable elements of photonic integrated circuits used to interconnect different optical devices, while avoiding the problems caused by undesired reflections of light in the circuit. They must, by necessity, have the form of a waveguide because they must be monolithically combined with other waveguide-based optical devices such as semiconductor lasers, optical amplifiers, and modulators. Conventional isolators, however, cannot meet this requirement because they use Faraday rotators and polarizers, which are difficult to integrate with waveguide-based semiconductor optical devices. For this reason, a lot of effort has been expended in developing waveguide isolators [1–6]. However, most reported devices use ferromagnetic garnets to ensure nonreciprocity in light propagation and, therefore, are incompatible with semiconductor optical devices.

One promising way of fabricating waveguide-based semiconductor isolators is by making use of the nonreciprocal-loss. In this phenomenon, the propaga-

0003-6935/07/235784-08$15.00/0
© 2007 Optical Society of America

tion loss of light in a semiconductor optical waveguide covered with a magnetized ferromagnetic layer is larger in backward propagation than it is in forward propagation [7,8]. This phenomenon can be used to develop semiconductor waveguide isolators that are suitable for monolithic integration with other semiconductor optical devices. The first example was reported by Vanwoleghem *et al.* [9,10]. Their device consists of an InGaAlAs/InP active waveguide with a ferromagnetic CoFe layer and operates in 1.3-μm TM mode.

To fabricate 1.5-μm band polarization-independent waveguide isolators, we developed both TE-mode and TM-mode isolators based on the nonreciprocal-loss phenomenon. First we fabricated a TE-mode isolator, consisting of an InGaAsP/InP active waveguide with a ferromagnetic Fe layer, and obtained a nonreciprocity of 14.7 dB/mm, the largest value ever reported for waveguide isolators [11,12]. We then turned to a TM-mode isolator and, in a previous paper, proposed the construction of a device with ferromagnetic manganese arsenide (MnAs) instead of Fe-based metals, and confirmed its nonreciprocal-loss operation with experiments at a 1.5-μm wavelength [13,14]. However, our prototype device had a simple gain-guiding structure with a small lateral-confinement factor and, therefore, left room for improvement. That is, the device showed a large forward propagation loss of 35–40 dB/mm, and was unable to operate in a single mode. To solve these problems, we changed the device's design to a ridge-waveguide structure with a large lateral-confinement factor. We designed the improved structure with the aid of electromagnetic simulation using the finite-difference method, and then fabricated devices with metal-organic vapor phase epitaxy. The device was able to operate in a single mode at 1.5 μm TM mode, with a reduced forward loss of 10.8 dB/mm. The nonreciprocity was 7.2 dB/mm and was almost constant at wavelengths from 1.53 to 1.55 μm. The following sections describe this improved TM-mode isolator in detail.

2. Structure of the Transverse-Magnetic-Mode Ridge Waveguide Isolator

Figure 1 is a cross-sectional diagram of our ridge waveguide isolator for 1.5-μm TM mode. The device consists of a TM-mode semiconductor optical amplifier (SOA) on an *n*-type InP substrate covered with a ferromagnetic manganese-arsenide (MnAs) layer. The SOA consists of a strained InGaAs/InGaAlAs multiple quantum well (MQW) sandwiched between two InGaAlAs guiding layers. The upper guiding layer is covered with a *p*-type InP cladding layer and a highly doped *p*-type InGaAs contact layer. These two layers separate the SOA from the MnAs layer, so together we call them a separation layer. The separation layer has to be thin so that light traveling in the SOA will extend into the MnAs layer to interact with the magnetization vector in the MnAs. An Au–Ti double metal layer on the MnAs layer forms a top electrode to supply a driving current to the SOA. An Al_2O_3 layer separates the SOA surface from the

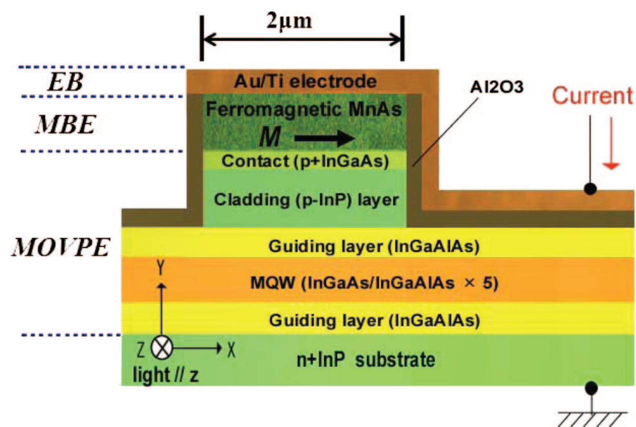

Fig. 1. (Color online) Schematic cross section of our waveguide isolator for 1.5-μm TM mode, consisting of a ridge-shaped optical amplifying waveguide covered with a MaAs layer magnetized in the x direction. Light propagates along the z direction.

Au–Ti electrode. Incident light passes through the SOA waveguide perpendicular to the figure (z direction).

To operate the device, an external magnetic field is applied so that the MnAs layer will be magnetized perpendicular to the propagation of light, as indicated by arrow M in the figure (x direction). Light traveling in the device interacts with the magnetized MnAs layer. This produces a difference in the TM mode effective refractive index of the device between forward (z direction) and backward propagation ($-z$ direction); therefore, the propagation loss is larger for backward propagation than it is for forward propagation. This nonreciprocal loss is caused by the magneto-optic transverse Kerr effect. The SOA compensates for the forward propagation loss; it is operated so that the net loss for forward propagation will be zero. Under these conditions, the device is able to act as an optical isolator.

In our device structure, which is dictated by the requirements of TM-mode operation, the ferromagnetic layer that produces the nonreciprocal loss is also used as a contact to supply a driving current to the SOA. This means that the ferromagnetic layer has to provide a low-resistance contact for the *p*-type InGaAs contact layer. To meet this requirement, we used MnAs for the ferromagnetic layer instead of ordinary ferromagnetic metals. MnAs is a ferromagnetic intermetallic compound with a hexagonal NiAs structure. It can be grown epitaxially on GaAs, InP, and related semiconductors using molecular beam epitaxy (MBE), without producing a solid-phase reaction at the interface [15,16]. MnAs is a suitable ferromagnetic material for our device because it has enough Kerr effect to produce practical nonreciprocity and, at the same time, unlike ordinary ferromagnetic metals such as Fe and Co, can make a low-resistance contact on the SOA waveguide without Schottky barriers on *p*-type InGaAs [17]. Although the Curie temperature of MnAs is a little low, at about 40 °C, it can be used stably in photonic in-

tegrated circuits because such circuits are generally used at controlled temperatures to operate laser diodes stably.

We designed a SOA structure for use at a 1.5-μm wavelength. The resultant structure is as follows: the substrate is a highly doped n-type InP (refractive index $n = 3.16$). The constituent layers of the SOAs are: (i) lower guiding layer: 100-nm-thick InGaAlAs (bandgap wavelength $\lambda_g = 1.1\ \mu$m, $n = 3.4$); (ii) MQW: five InGaAs quantum wells (-0.4% tensile-strained, 15-nm-thick well, $n_{MQW} = 3.53$) with six InGaAlAs barriers ($+0.6\%$ compressively strained, 12-nm-thick barrier, $\lambda_g = 1.2\ \mu$m); and (iii) upper guiding layer: 100-nm-thick InGaAlAs ($\lambda_g = 1.1\ \mu$m). The ridge waveguide's width was set at 2 μm to operate the device in a single mode.

The thickness of the separation (InP cladding layer plus the InGaAs contact layer) and MnAs layers affects the strength of interaction between light traveling through the SOA and the magnetization vector in the MnAs layer. Therefore, we determined the optimum thickness of these two layers using the calculation in Section 3.

3. Determining Layer Thickness

In our isolator, light traveling along the SOA waveguide extends through the separation layer into the MnAs layer to a certain penetration depth, and interacts with magnetic moments in the MnAs layer to ensure nonreciprocity. Therefore, the thickness of the separation layer and the MnAs layer greatly affect performance—the isolation ratio and the forward loss (insertion loss) of the isolator—as follows:

(i) A large isolation ratio can be obtained at a small separation-layer thickness because a thin separation layer easily lets light into the MnAs layer to produce a large optomagnetic interaction. However, a thin separation layer also increases the amount of light absorbed in the MnAs layer (MnAs is not sufficiently transparent for 1.5-μm light) thereby increasing the insertion loss of the isolator. The separation layer should be thin as long as the amplifying gain of the SOA can compensate for the absorption loss of light in the MnAs layer.

(ii) The MnAs layer has to be thicker than the penetration depth of light in MnAs. If it is not, light leaks out of the MnAs layer and is absorbed by the Au–Ti electrode. This increases forward loss and reduces the isolation ratio. Therefore, a larger thickness is better for the MnAs layer. However, it is difficult to grow a high-quality MnAs layer with a thickness of more than 300–400 nm using existing epitaxial process technology [18]. During the device's design phase, it must be ascertained whether the device will perform adequately with a thin MnAs layer.

To determine the optimum thickness of the separation and MnAs layers, we calculated the isolation ratio and the insertion loss of the device as a function of these thicknesses by means of a two-dimensional electromagnetic simulation based on the finite-difference method (FDM). The details of this simulation are described in Appendix A.

Figure 2 summarizes the results, i.e., the absorption loss for forward and backward propagation together with the isolation ratio as a function of the MnAs layer thickness, with the separation-layer thickness as a parameter. The device's absorption loss is large and the isolation ratio is small at small MnAs thickness because part of the propagating light in the device leaks out of the MnAs layer and is needlessly absorbed by the Au–Ti electrode. As MnAs layer thickness increases, absorption loss decreases and isolation ratio increases; both approach a con-

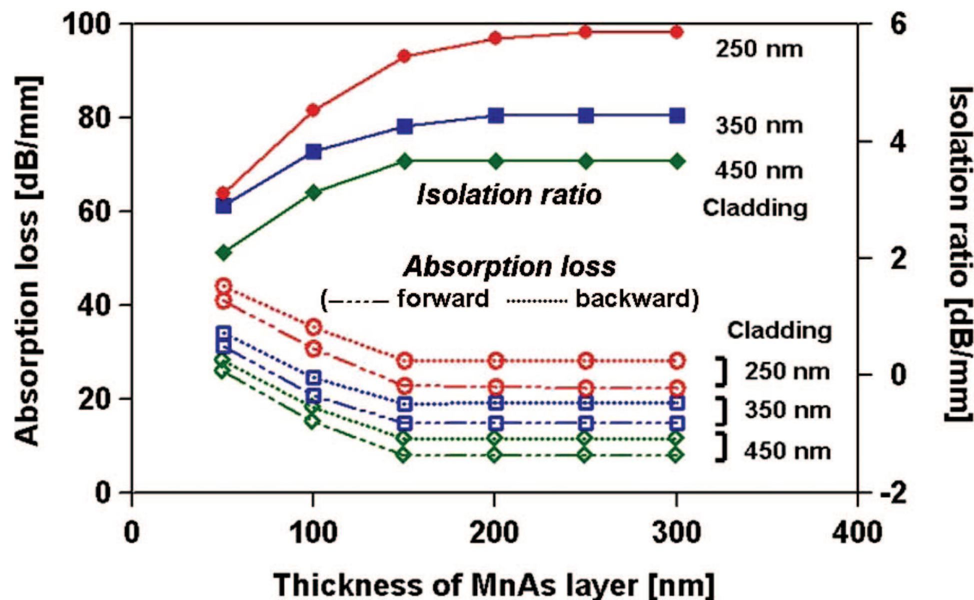

Fig. 2. (Color online) Forward and backward absorption loss (propagation loss) and isolation ratio (nonreciprocity) in the device as a function of MnAs-layer thickness and cladding layer thickness, calculated for 1.55-μm TM mode.

stant in MnAs layers thicker than 200 nm. This means that light penetrates to a depth of about 200 nm in the MnAs layer. Therefore, 200 nm can be considered a necessary and sufficient thickness for the MnAs layer when fabricating the devices. This thickness is practical; we can grow a 200-nm-thick MnAs layer on an InGaAs contact layer by means of MBE. We decided to set the MnAs thickness to 200 nm.

Figure 2 also shows that both the isolation ratio and the absorption loss increase as the separation layer thickness decreases. This is because a thinner separation layer lets a higher percentage of light through into the MnAs layer, producing a larger interaction. A thin separation layer is preferable for obtaining a large isolation ratio as long as the forward absorption loss can be compensated for by the amplifying gain of the SOA. Because we expected that an SOA gain of 16 dB/mm could be achieved, we decided to set the separation layer thickness to 350 nm.

Figure 3 shows the distribution profile of light traveling in the isolator for forward and backward propagation, as we calculated for a device with a 350-nm separation layer and a 200-nm MnAs layer. Figures 3(a-1) and 3(b-1) show the contour lines for TM magnetic field vector intensity—large magnetic fields in the central part—on the cross section (x–y plane) of the device: Fig. 3(a-1) is for forward propagating light, and Fig. 3(b-1) is for backward light. Figures 3(a-2) and 3(b-2) depict the magnetic field vector intensity along the vertical center line [dashed lines in Figs. 3(a-1) and 3(b-1)] of the device; Fig. 3(a-2) is for forward light, and Fig. 3(a) is for backward light. As the figures show, unlike forward propagating light, backward propagating light shifts its distribution tail to the MnAs layer and, therefore, suffers a larger absorption loss in the MnAs layer. That is, the propagation loss of light is larger in backward propagation than it is in forward propagation.

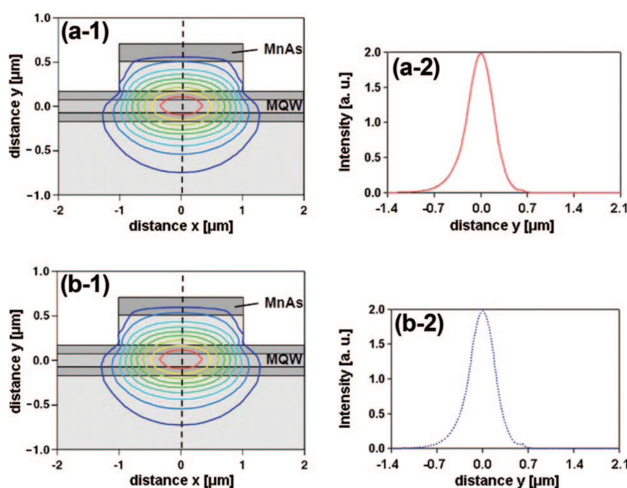

Fig. 3. (Color online) Distribution profile of light traveling in the isolator, calculated for 1.55-μm TM mode, with a 350-nm cladding layer and a 200-nm MnAs layer: cross section of distribution for (a-1) forward and (b-1) backward propagating light; distribution along vertical center line [dashed lines in (a-1) and (b-1)] of the device for (a-2) forward and (b-2) backward propagating light.

4. Fabricating the Device

On the basis of the results obtained in the previous sections, we fabricated actual devices in the following manner: the substrate was a highly doped, [100]-oriented n-type wafer of InP. The SOA was formed on the substrate, using metal-organic vapor phase epitaxy (MOVPE). The MQW showed a photoluminescence peak at 1.54 μm—this means that the SOA had a gain peak at 1.54 μm. The thickness of the InP cladding layer and the InGaAs contact layer were set to 350 nm and 10 nm, respectively. After the formation of the SOA, by means of MBE, a 200-nm MnAs layer was grown on the surface of the InGaAs contact layer with a growth rate of 80 nm/h. We observed the surface of the layer with a high-energy-electron-diffraction pattern during the growth process and confirmed the (1×2) reconstruction (the structural characteristic of single crystalline MnAs).

After the growth of MnAs, the ridge-waveguide structure was formed as follows. First, a photoresist mask in the form of a 2-μm-wide waveguide pattern was made on the surface of the MnAs layer. Then, the MnAs, InP cladding layer, and InGaAs contact layers were selectively etched in this order to fabricate a ridge waveguide; the MnAs layer was etched by reactive ion etching with Ar, and the cladding and the contact layers were wet-etched with a Br_2-HBr-H_2O solution. A 100-nm Al_2O_3 layer was deposited on this ridge waveguide using electron-beam (EB) evaporation. Then, the Al_2O_3 on the contact layer was removed using a lift-off process. Finally, a 100-nm Ti layer and a 200-nm Au layer were deposited to make a top electrode, using EB evaporation. This was the process we used to fabricate the structure that is depicted in Fig. 1. Finally, both ends of the device were cleaved, and the cleaved surfaces were left uncoated. Figure 4 is a cross section of the device as observed with scanning electron microscopy (SEM).

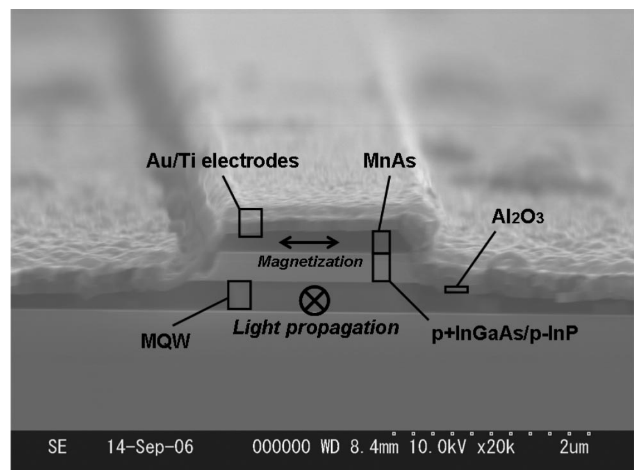

Fig. 4. SEM cross section of the device.

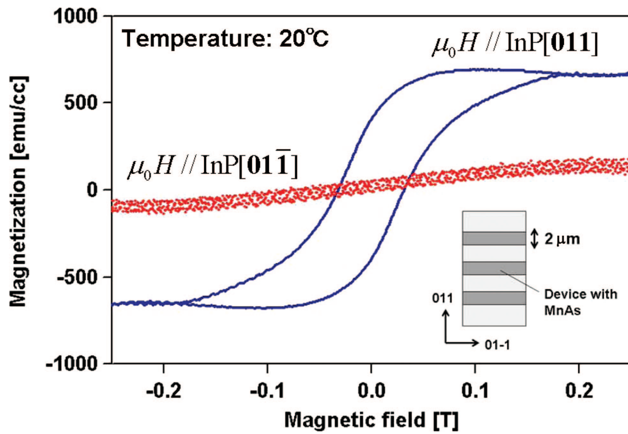

Fig. 5. (Color online) Magnetization curve for MnAs layer, measured with an AGFM. MnAs layer can be easily magnetized along the [011] direction of the InP substrate. In contrast, magnetization is difficult along the [01-1] direction.

The MnAs layer on the InGaAs contact layer showed strong magnetocrystalline anisotropy (an intrinsic property of ferromagnetic crystals). In our device, this magnetocrystalline anisotropy is stronger than the shape anisotropy. Figure 5 is a plot of the magnetization curve of the MnAs layer grown on the device, that is measured with alternating gradient force magnetometry (AGFM). Along the [011] direction of the InP substrate, the MnAs layer showed an easy-magnetization curve with a small coercive field of 0.07 T. In contrast, the magnetization was not easy along the [01-1] direction and was insufficient even in a magnetic field of 0.5 T. Therefore, to operate the device with a small external field, we formed the waveguide stripe parallel to the [0-11] direction of the InP substrate and magnetized the MnAs layer along the [011] direction with an external magnetic field of 0.07–0.1 T (initial magnetizing requires 0.15–0.2 T).

5. Device Operation

We confirmed that the device functioned successfully as an optical isolator with nonreciprocal loss for TM-polarized 1.5-μm light. Figure 6 shows our experimental setup for the measurement. It consisted of a wavelength-tunable laser, polarization controllers, two circulators and two switches, an output coupler, an optical power meter, and an optical spectrum analyzer (OSA). Light from a tunable laser was transmitted to the device through a polarization controller and a circulator. The light was transferred into and out of the device using lensed-fiber couplers. A magnetic field was applied using a permanent magnet along the [011] direction of the device, i.e., parallel to the surface of the device and perpendicular to the direction of light propagation (see Fig. 1). Light propagation in the device was switched between the forward direction (switch node 1–upper circulator–device–lower isolator–switch node 4 in Fig. 6) and backward direction (node 2–lower circulator–device–upper isolator–node 3) by controlling the optical switches. The intensity of light transmitted in the device (or the output light from the device) was measured using the optical spectrum analyzer and the power meter. The output of the tunable laser was set to 5 dBm, and the magnetic field for the device was set to 0.1 T. During measurement, the device was kept at 20 °C and operated with a driving current of 100 mA (current density = 2.5 kA/cm^2). The voltage drop across the device was 1.7 V—a small voltage drop due to the fact that, unlike ordinary ferromagnetic metal such as Fe and Ni, MnAs can provide a low-resistance contact for the InGaAs contact layer [17].

Figure 7 shows transmission spectra of the device with a length of 0.65 mm. The intensity of the output light from the device is plotted as a function of wavelength for forward (dashed line) and backward (solid line) propagation of (a) TM-polarized and (b) TE-polarized light. The wavelength of incident light was fixed at 1.54 μm, which was the gain peak wavelength of the SOA. For TM-mode light, the output intensity changed by 4.7 dB by switching the direction of light propagation. The device operated efficiently as a TM-mode isolator with an isolation ratio of 7.2 dB/mm (= 4.7 dB/0.65 mm). In contrast, the output intensity for TE-mode light was not dependent on the direction of the light propagation. Figure 7 also shows small periodic ripples in amplified spontaneous emission spectra. The interval of the periodic ripples corresponds to the Fabry–Perot interference by the cleaved facets, according to the length and effective refractive index of the device. The inset in Fig. 7(a) is the near-field pattern of the TM-mode

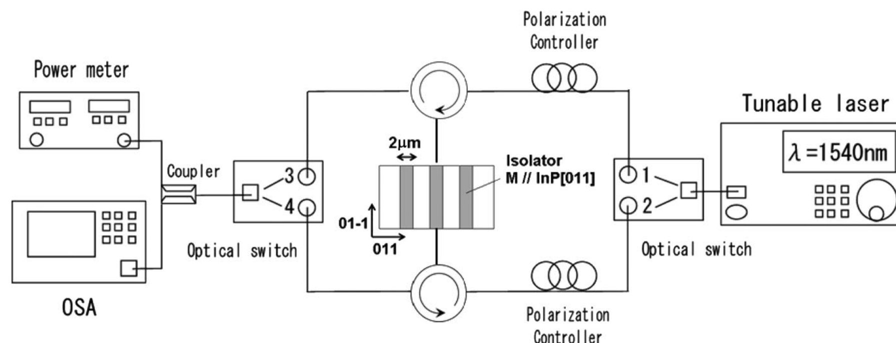

Fig. 6. Experimental setup for measuring isolation ratio and propagation loss of light in the device.

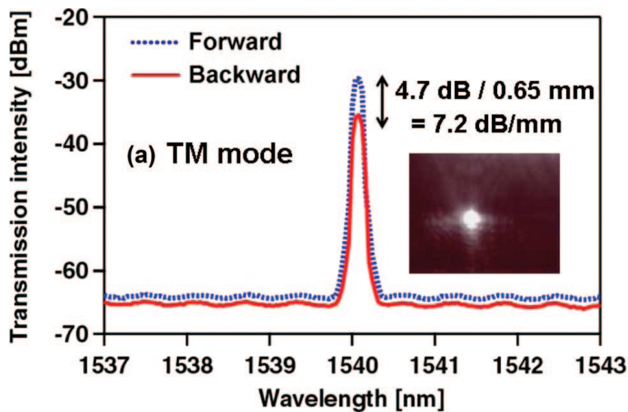

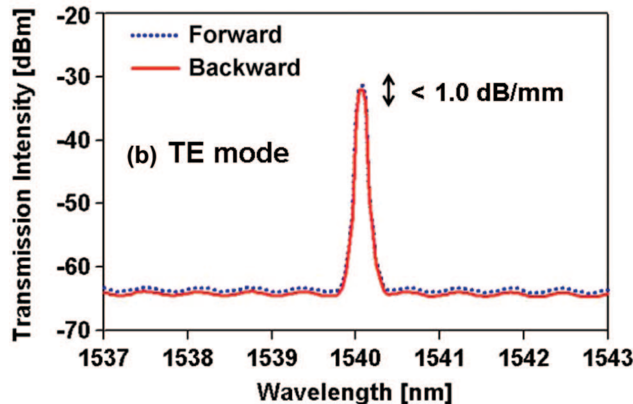

Fig. 7. (Color online) Transmission spectra of device for forward transmission (dashed curve) and backward transmission (solid curve), measured for (a) TM mode and (b) TE mode, at 1.54-μm wavelength, 100-mA driving current, and 0.1-T magnetic field. The device is 0.65 mm long. Data on transmission intensity include loss caused by the measurement system. Inset is the near-field pattern of the TM-mode forward propagating light.

forward propagating light and shows that the device operated successfully in a single mode.

The data of transmission intensity in Fig. 7 include the loss caused by the measurement system, i.e., the loss caused mainly by lensed-fiber couplers and the

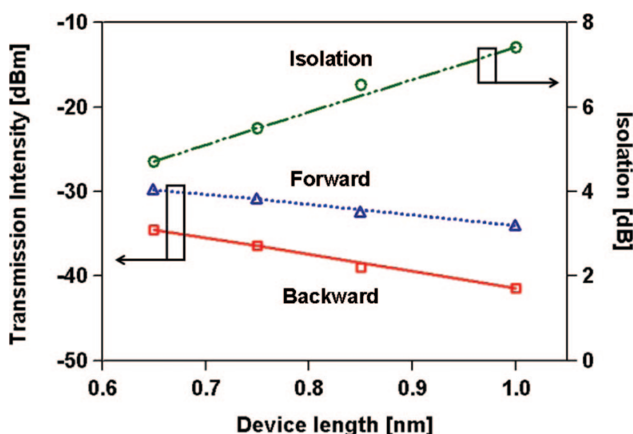

Fig. 8. (Color online) Transmission intensity as a function of device length, measured for the 1.54-μm TM mode, with 100-mA driving current and 0.1-T magnetic field. The isolation ratio is also plotted.

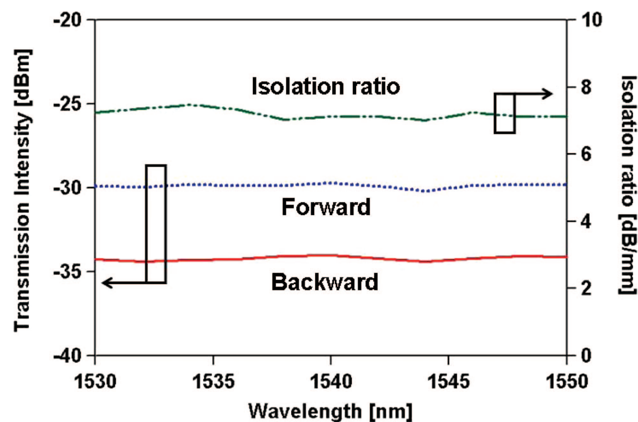

Fig. 9. (Color online) Isolation ratio as a function of a wavelength from 1.53 to 1.55 μm for a 0.65-mm long device. The transmission intensity is also plotted for forward and backward propagation (including measurement system loss).

output coupler. To examine the device's intrinsic transmission loss, we measured the transmission intensity for devices with different lengths. Figure 8 shows the results, i.e., the output intensity for forward and backward transmission as a function of device length (isolation ratio is also plotted). The slope of the forward line gives the intrinsic transmission loss (or absorption loss) per unit length, and we estimated that forward loss in the device was 10.6 dB/mm—far smaller than that in our previous device with a gain-guiding structure ($\sim$ 35 dB/mm). The loss caused by the measurement system can be calculated using the vertical-axis intercept of the forward line and the output intensity of the tunable laser. It was estimated to be 28 dB—output coupler loss = 3 dB plus the loss of lensed-fiber coupling between the measurement system and the device = 12.5 dB/facet $\times$ 2.

Figure 9 is a plot of the isolation ratio, as a function of wavelength from 1.53 to 1.55 μm. The device was 0.65-mm long. The output intensities for forward and backward propagations are also plotted (including the measurement system loss). In this range of wavelength, the isolation ratio was almost constant.

The forward transmission loss (i.e., insertion loss) of this ridge-waveguide isolator was much less than with our previous gain-guiding waveguide isolators but was still too large for practical use. This is so because the gain of the SOA was lower than we had expected, and therefore, insufficient to compensate for the intrinsic transmission loss in the device. Increasing the number of well layers in the MQW region is an effective way of improving the SOA gain. To reduce the forward loss to 1 dB/mm or less, we are now fabricating ridge-waveguide isolators with twice as many MQW wells. With this improved structure, we will be able make low-loss waveguide isolators and proceed to develop photonic integrated circuits.

6. Conclusion

We fabricated a 1.5-μm TM-mode waveguide isolator. To improve our previous gain guiding device which

showed large insertion loss (~ 35 dB/mm) and a lateral multimode propagation, our device, which we believe is novel, formed a ridge SOA waveguide with a ferromagnetic MnAs layer. The MnAs layer serves a dual function of producing the nonreciprocal loss phenomenon due to its magneto-optic effect and of acting as a low-resistance contact on the semiconductor waveguide. The thicknesses of the cladding layer and the MnAs layer affect the nonreciprocal performance and insertion loss in the device. Therefore, by using FDM simulation, we first estimated the optimum thicknesses of these layers for a 1.5-μm operation. On the basis of this simulation, we fabricated an actual ridge waveguide device which had a reduced insertion loss (~ 10.6 dB/mm) and a lateral single-mode operation. The device showed a stable nonreciprocal loss (or isolation ratio) of 7.2 dB/mm from 1.53 μm to 1.55 μm TM mode.

Appendix A

The nonreciprocity of our isolator is caused by the off-diagonal elements in the dielectric tensor of the ferromagnetic MnAs. The dielectric tensor of each layer in the isolator (see Fig. 1) is given by

$$\begin{pmatrix} \varepsilon_n & 0 & 0 \\ 0 & \varepsilon_n & j\alpha \\ 0 & -j\alpha & \varepsilon_n \end{pmatrix}, \tag{A1}$$

where ε_n is the diagonal element of the tensor in nth layer. The off-diagonal element α is 0 except in the MnAs layer. Using these tensors and Maxwell's equations, we obtain the scalar wave equation for magnetic field H_x (parallel to x axis) of the TM waves in each layer. The wave equation in the semiconductor layers and the Au–Ti layer is given by

$$\frac{\partial^2 H_x}{\partial x^2} + \frac{\partial^2 H_x}{\partial y^2} + AH_x = 0 \quad (A = k_0{}^2\varepsilon_n - \beta^2), \tag{A2}$$

where $k_0{}^2 = \omega^2\mu_0\varepsilon_0 = (2\pi/\lambda)^2$ is the free-space propagation constant and β is the propagation constant in the device along z direction. For the MnAs layer, the wave equation has first-order and third-order derivative terms because of the nonzero off-diagonal element α in the dielectric tensor. For the α value of MnAs, third-order terms are small and can be ignored. In consequence, the wave equation in the MnAs layer is given by

$$\frac{\partial^2 H_x}{\partial x^2} + \frac{\partial^2 H_x}{\partial y^2} - \frac{\varepsilon_n}{\alpha\beta} B \frac{\partial H_x}{\partial y} + BH_x = 0$$

$$\left(B = k_0{}^2\varepsilon_n - \beta^2 - \frac{k_0{}^2\alpha^2}{\varepsilon_n}\right). \tag{A3}$$

The first-order derivative term produces a difference in an effective extinction coefficient between forward (z direction) and backward ($-z$ direction) TM waves, thereby producing the optical nonreciprocity in our isolator.

To solve the wave equation numerically, we partition the domain in space using a mesh $x_0, x_1, \ldots x_p, \ldots$ in the x direction and mesh $y_0, y_1, \ldots y_q, \ldots$ in the y direction with a mesh width (the difference between two adjacent space points) of m in the x direction and n in the y direction. We represent the magnetic field on each mesh point (x_p, y_q) by $H_{p,q}$. Using a second-order central difference for the space derivative at position (x_p, y_q), we obtain recurrence equation

$$\frac{1}{m^2}H_{p-1,q} + \frac{1}{m^2}H_{p+1,q} + \frac{1}{n^2}H_{p,q-1} + \frac{1}{n^2}H_{p,q+1} + \left(A - \frac{2}{m^2} - \frac{2}{n^2}\right)H_{p,q} = 0, \tag{A4}$$

for Eq. (A2), and recurrence equation

$$\frac{1}{m^2}H_{p-1,q} + \frac{1}{m^2}H_{p+1,q} + \frac{1}{n^2}H_{p,q-1} + \frac{\varepsilon_n}{2n\alpha\beta}BH_{p,q-1} + \frac{1}{n^2}H_{p,q+1} - \frac{\varepsilon_n}{2n\alpha\beta}BH_{p,q+1} + \left(B - \frac{2}{m^2} - \frac{2}{n^2}\right)H_{p,q} = 0, \tag{A5}$$

for Eq. (A3). We solved Eqs. (A4) and (A5) numerically to calculate forward and backward propagation loss and an isolation ratio, as a function of the thickness of the separation layer and the MnAs layer, for 1.55-μm TM mode, where the SOA was not operated (i.e., driving current = 0). The dielectric tensor parameters we used are given in Table 1; the data for MnAs are from our previous paper [14]. In our calculations, we assumed that H_x showed an exponential attenuation in the Au–Ti electrode and the InP substrate and followed the Dirichlet condition ($H_x = 0$) in the Al_2O_3 insulating layer. We also assumed the thickness of the contact layer to be 0; this is not a problem because, in our actual devices, the contact layer was far thinner than the cladding layer (see Section 4).

Table 1. Parameters Used for Calculating Device Characteristics

Parameters	Values	Layers
ε_1, ε_5	$(3.16)^2$	InP substrate, InP cladding layer
ε_2, ε_4	$(3.4)^2$	InGaAsP down, upper guiding layer[a]
ε_3	$(3.53)^2$	MQW layer[b]
ε_6	$(2.8 + 4i)^2$	Ferromagnetic MnAs layer
ε_7	$(0.6 + 10i)^2$	Au/Ti metal electrode
α	$-1.62 + 0.27i$	Ferromagnetic MnAs layer
m	200×10^{-9}	Mesh width of x axis
n	50×10^{-9}	Mesh width of y axis

[a]The thickness of each guiding layer is fixed to 100 nm.
[b]The thickness of the MQW layer is fixed to 150 nm.

References

1. M. Levy, R. M. Osgood, H. Hegde, F. J. Cadieu, R. Wolfe, and V. J. Fratello, "Integrated optical isolators with sputter-deposited thin-film magnets," IEEE Photon. Technol. Lett. **8,** 903–905 (1996).
2. H. Yokoi, T. Mizumoto, N. Shinjo, N. Futakuchi, and Y. Nakano, "Demonstration of an optical isolator with a semiconductor guiding layer that was obtained by use of a nonreciprocal phase shift," Appl. Opt. **39,** 6158–6164 (2000).
3. J. Fujita, M. Levy, R. M. Osgood, L. Wilkens, and H. Dotsch, "Waveguide optical isolator based on Mach-Zehnder interferometer," Appl. Phys. Lett. **76,** 2158–2160 (2000).
4. V. Zayets, M. C. Debnath, and K. Ando, "Optical isolation in $Cd_{1-x}Mn_xTe$ magneto-optical waveguide grown on GaAs substrate," Jpn. J. Appl. Phys., Part 2 **43,** L1561–L1563 (2004).
5. J. S. Yang, J. W. Roh, S. H. Ok, D. H. Woo, Y. T. Byun, W. Y. Lee, T. Mizumoto, and S. Lee, "An integrated optical waveguide isolator based on multimode interference by wafer direct bonding," IEEE Trans. Magn. **41,** 3520–3522 (2005).
6. Y. Shoji and T. Mizumoto, "Wideband design of nonreciprocal phase shift magneto-optical isolators using phase adjustment in Mach-Zehnder interferometers," Appl. Opt. **45,** 7144–7150 (2006).
7. M. Takenaka and Y. Nakano, "Proposal of a novel semiconductor optical waveguide isolator," in *Proceedings of IEEE Conference on Indium Phosphide and Related Materials* (IEEE, 1999), pp. 289–292.
8. W. Zaets and K. Ando, "Optical waveguide isolator based on nonreciprocal loss/gain of amplifier covered by ferromagnetic layer," IEEE Photon. Technol. Lett. **11,** 1012–1014 (1999).
9. M. Vanwolleghem, W. Van Parys, D. Van Thourhout, R. Baets, F. Lelarge, O. Gauthier-Lafaye, B. Thedrez, R. Wirix-Speetjens, and L. Lagae, "Experimental demonstration of nonreciprocal amplified spontaneous emission in a CoFe clad semiconductor optical amplifier for use as an integrated optical isolator," Appl. Phys. Lett. **85,** 3980–3982 (2004).
10. W. Van Parys, B. Moeyersoon, D. Van Thourhout, R. Baets, M. Vanwolleghem, B. Dagens, J. Decobert, O. L. Gouezigou, D. Make, R. Vanheertum, and L. Lagae, "Transverse magnetic mode nonreciprocal propagation in an amplifying AlGaInAs/InP optical waveguide isolator," Appl. Phys. Lett. **88,** 071115 (2006).
11. H. Shimizu and Y. Nakano, "First demonstration of TE mode nonreciprocal propagation in an InGaAsP/InP active waveguide for an integratable optical isolator," Jpn. J. Appl. Phys., Part 2 **43,** L1561–L1563 (2004).
12. H. Shimizu and Y. Nakano, "Fabrication and characterization of an InGaAsp/InP active waveguide optical isolator with 14.7 dB/mm TE mode nonreciprocal attenuation," IEEE J. Lightwave Technol. **24,** 38–43 (2006).
13. T. Amemiya, H. Shimizu, Y. Nakano, P. N. Hai, M. Yokoyama, and M. Tanaka, "Semiconductor waveguide optical isolator based on nonreciprocal loss induced by ferromagnetic MnAs," Appl. Phys. Lett. **89,** 021104 (2006).
14. T. Amemiya, H. Shimizu, P. N. Hai, M. Yokoyama, M. Tanaka, and Y. Nakano, "Waveguide-based 1.5-μm optical isolator based on magneto-optic effect in ferromagnetic MnAs," Jpn. J. Appl. Phys., Part 1 **46,** 205–210 (2007).
15. M. Tanaka, J. P. Harbison, T. Sands, T. L. Cheeks, and G. M. Rothberg, "Molecular-beam epitaxy of MnAs thin-films on GaAs," J. Vac. Sci. Technol. B **12,** 1091–1094 (1994).
16. M. Yokoyama, S. Ohya, and M. Tanaka, "Growth and magnetic properties of epitaxial MnAs thin films grown on InP(001)," Appl. Phys. Lett. **88,** 012504 (2006).
17. T. Amemiya, H. Shimizu, and Y. Nakano, "TM mode waveguide optical isolator based on the nonreciprocal loss shift," in *Proceedings of IEEE Conference on Indium Phosphide and Related Materials* (IEEE, 2005), pp. 303–306.
18. L. Daweritz, L. Wan, B. Jenichen, C. Herrmann, J. Mohanty, A. Trampert, and K. H. Ploog, "Thickness dependence of the magnetic properties of MnAs films on GaAs(001) and GaAs(113)A: Role of a natural array of ferromagnetic stripes," J. Appl. Phys. **96,** 5056–5052 (2004).